Spectrally encoded spectral imaging

Avraham Abramov, Limor Minai and Dvir Yelin*

Department of Biomedical Engineering, Technion – Israel Institute of Technology, Technion City 32000, Haifa, Israel
**yelin@bm.technion.ac.il*

Abstract: Spectral imaging, i.e. the acquisition of the spectrum emitted from each sample location, is a powerful tool for a wide variety of applications in science and technology. For biomedical applications, spectral imaging is important for accurate analysis of a biological specimen and for assisting clinical diagnosis, however it could be challenging mainly due to the typically low damage thresholds and strict time constraints. Here, we present a fiber-based technique termed spectrally encoded spectral imaging (SESI), in which a fully emitted spectrum is captured from each resolvable point of a specimen using an additional lateral scanning of the spectrally encoded line. The technique is demonstrated by capturing spectral data cubes of a color print and of a green leaf, and its potential advantage in signal-to-noise ratio is theoretically discussed. Using a miniaturized grating-lens configuration, SESI could be conducted endoscopically, allowing minimally invasive color and spectral imaging in remote locations of the body.

OCIS codes: (110.4234) Multispectral and hyperspectral imaging; (170.2150) Endoscopic imaging; (060.2350) Fiber optics imaging; (330.1710) Color measurement.

References and links

1. N. Gat, "Imaging spectroscopy using tunable filters: A review," Proc. SPIE **4056**, 50–64 (2000).
2. R. D. Shonat, E. S. Wachman, W. H. Niu, A. P. Koretsky, and D. L. Farkas, "Near-simultaneous hemoglobin saturation and oxygen tension maps in mouse brain using an AOTF microscope," Biophys. J. **73**(3), 1223–1231 (1997).
3. Q. S. Hanley, P. J. Verveer, D. J. Arndt-Jovin, and T. M. Jovin, "Three-dimensional spectral imaging by hadamard transform spectroscopy in a programmable array microscope," J. Microsc. **197**(1), 5–14 (2000).
4. X. H. Gao, Y. Y. Cui, R. M. Levenson, L. W. K. Chung, and S. M. Nie, "In vivo cancer targeting and imaging with semiconductor quantum dots," Nat. Biotechnol. **22**(8), 969–976 (2004).
5. M. B. Sinclair, J. A. Timlin, D. M. Haaland, and M. Werner-Washburne, "Design, construction, characterization, and application of a hyperspectral microarray scanner," Appl. Opt. **43**(10), 2079–2088 (2004).
6. Y. Garini, I. T. Young, and G. McNamara, "Spectral imaging: principles and applications," Cytometry A **69A**(8), 735–747 (2006).
7. Z. Malik, M. Dishi, and Y. Garini, "Fourier transform multipixel spectroscopy and spectral imaging of protoporphyrin in single melanoma cells," Photochem. Photobiol. **63**(5), 608–614 (1996).
8. E. Schröck, S. du Manoir, T. Veldman, B. Schoell, J. Wienberg, M. A. Ferguson-Smith, Y. Ning, D. H. Ledbetter, I. Bar-Am, D. Soenksen, Y. Garini, and T. Ried, "Multicolor spectral karyotyping of human chromosomes," Science **273**(5274), 494–497 (1996).
9. T. Zimmermann, J. Rietdorf, and R. Pepperkok, "Spectral imaging and its applications in live cell microscopy," FEBS Lett. **546**(1), 87–92 (2003).
10. I. Barshack, J. Kopolovic, Z. Malik, and C. Rothmann, "Spectral morphometric characterization of breast carcinoma cells," Br. J. Cancer **79**(9/10), 1613–1619 (1999).
11. D. L. Farkas and D. Becker, "Applications of spectral imaging: detection and analysis of human melanoma and its precursors," Pigment Cell Res. **14**(1), 2–8 (2001).
12. F. Jean, G. Bourg-Heckly, and B. Viellerobe, "Fibered confocal spectroscopy and multicolor imaging system for in vivo fluorescence analysis," Opt. Express **15**(7), 4008–4017 (2007).
13. H. Makhlouf, A. F. Gmitro, A. A. Tanbakuchi, J. A. Udovich, and A. R. Rouse, "Multispectral confocal microendoscope for in vivo and in situ imaging," J. Biomed. Opt. **13**(4), 044016 (2008).
14. A. Chung, S. Karlan, E. Lindsley, S. Wachsmann-Hogiu, and D. L. Farkas, "In vivo cytometry: A spectrum of possibilites," Cytometry A **69A**(3), 142–146 (2006).

#141151 - $15.00 USD Received 14 Jan 2011; revised 6 Mar 2011; accepted 6 Mar 2011; published 25 Mar 2011

15. M. E. Martin, M. B. Wabuyele, K. Chen, P. Kasili, M. Panjehpour, M. Phan, B. Overholt, G. Cunningham, D. Wilson, R. C. Denovo, and T. Vo-Dinh, "Development of an advanced hyperspectral imaging (HSI) system with applications for cancer detection," Ann. Biomed. Eng. **34**(6), 1061–1068 (2006).
16. C. M. Brown, P. G. Reinhall, S. Karasawa, and E. J. Seibel, "Optomechanical design and fabrication of resonant microscanners for a scanning fiber endoscope," Opt. Eng. **45**(4), 043001 (2006).
17. C. M. Lee, C. J. Engelbrecht, T. D. Soper, F. Helmchen, and E. J. Seibel, "Scanning fiber endoscopy with highly flexible, 1 mm catheterscopes for wide-field, full-color imaging," J Biophotonics **3**(5-6), 385–407 (2010).
18. E. J. Seibel, R. E. Carroll, J. A. Dominitz, R. S. Johnston, C. D. Melville, C. M. Lee, S. M. Seitz, and M. B. Kimmey, "Tethered capsule endoscopy, a low-cost and high-performance alternative technology for the screening of esophageal cancer and Barrett's esophagus," IEEE Trans. Biomed. Eng. **55**(3), 1032–1042 (2008).
19. G. J. Tearney, R. H. Webb, and B. E. Bouma, "Spectrally encoded confocal microscopy," Opt. Lett. **23**(15), 1152–1154 (1998).
20. D. Kang, D. Yelin, B. E. Bouma, and G. J. Tearney, "Spectrally-encoded color imaging," Opt. Express **17**(17), 15239–15247 (2009).
21. A. Abramov, L. Minai, and D. Yelin, "Multiple-channel spectrally encoded imaging," Opt. Express **18**(14), 14745–14751 (2010).
22. M. Merman, A. Abramov, and D. Yelin, "Theoretical analysis of spectrally encoded endoscopy," Opt. Express **17**(26), 24045–24059 (2009).
23. D. Yelin, W. M. White, J. T. Motz, S. H. Yun, B. E. Bouma, and G. J. Tearney, "Spectral-domain spectrally-encoded endoscopy," Opt. Express **15**(5), 2432–2444 (2007).
24. J. T. Motz, D. Yelin, B. J. Vakoc, B. E. Bouma, and G. J. Tearney, "Spectral- and frequency-encoded fluorescence imaging," Opt. Lett. **30**(20), 2760–2762 (2005).
25. M. Strupler, E. D. Montigny, D. Morneau, and C. Boudoux, "Rapid spectrally encoded fluorescence imaging using a wavelength-swept source," Opt. Lett. **35**(11), 1737–1739 (2010).
26. D. Yelin, I. Rizvi, W. M. White, J. T. Motz, T. Hasan, B. E. Bouma, and G. J. Tearney, "Three-dimensional miniature endoscopy," Nature **443**(7113), 765–765 (2006).

1. Introduction

The optical spectrum emitted from a specimen carries invaluable information regarding its structure, chemical composition and physical parameters. Spectral imaging, a combination of imaging and spectroscopy, provides three dimensional spectral cubes which contain the spectra of all the points of the imaged object. Spectral imaging has been shown useful for a wide variety of applications, including earth sciences, oceanography, homeland security, the food industry, as well as for biological and clinical applications.

Optical techniques for acquiring full spectral images often include a wavelength dependant optical module and an imaging system for capturing spectral information. Due to the large amount of acquired data, a main challenge of spectral imaging is the total measurement time required to complete the acquisition of a full data set. In its most basic form, spectral imaging is accomplished by successively acquiring a series of images through different color filters [1–4]. Other approaches for capturing spectral cubes employ wavelength dispersion using diffractive elements such as gratings and prisms. These methods often require scanning of the specimen point-by-point or in sequential lines [5]. The total acquisition time frames using these approaches depend on the specific scanning mechanism used and on the signal-to-noise ratio (SNR), which in many applications is limited due to the maximum light intensity that the sample could tolerate without being damaged. Using low coherence interferometry, spectral imaging with significantly higher SNR was demonstrated, in which spectral information was extracted by calculating the Fourier transform of three-dimensional interferograms acquired while scanning the optical path of a reference image [6,7].

In the biomedical research, spectral imaging was demonstrated useful for a wide variety of applications, including spectral karyotyping [8], live cell imaging [9], and the characterization of breast carcinoma cells [10]. For *in vivo* clinical applications, spectral imaging could be difficult to perform due to practical concerns such as the maximum tolerated light intensity and the restricted imaging time. While the skin surface is relatively accessible and allows effective non-invasive spectral imaging [11], internal organs require specific endoscopic instrumentation for effective imaging. Fiber bundle endoscopy was demonstrated capable of *in vivo* fluorescence analysis [12,13] and hyperspectral imaging of early stages of cancer by using a wavelength swept source [14] or a liquid crystal tunable filter [15]. Recently, a single

#141151 - $15.00 USD Received 14 Jan 2011; revised 6 Mar 2011; accepted 6 Mar 2011; published 25 Mar 2011

fiber endoscope that uses rapid distal scanning [16,17] was demonstrated promising for the screening of esophageal cancer and Barrett's esophagus using spectral imaging with multi wavelength illumination and color sensitive detection [18].

Spectrally encoded confocal microscopy (SECM) and spectrally encoded endoscopy (SEE), first presented by Tearney *et al.* [19], are minimally invasive, single fiber imaging techniques which utilize a dispersive element and a lens to angularly disperse and focus a broadband light to a transverse line on a specimen. In this approach, the reflected spectrally encoded light is collected by a single fiber and measured by a spectrometer for mapping the spatial reflectance. A two dimensional image is formed by slowly scanning the spectrally encoded line across the sample, for example, by rotating the imaging probe. Since only a single wavelength is detected from each point on the sample, spectrally encoded imaging is not suitable for spectral imaging at its most basic form of image acquisition; moreover, colored specimens would appear with visible local artifacts as a result of the space-wavelength encoding process. Recently, this problem was addressed by demonstrating color-sensitive SECM system [20] which utilized three optical fibers to simultaneously illuminate each point on the sample with three wavelengths from the red, green and blue parts of the spectrum. While this method would allow real-time color imaging without additional scanning, its color vision is still limited toward the edges of the frame, and the field of view is often restricted since only a small portion (approximately one third) of the entire spectrum is used for spatial encoding.

In this paper we show that by using an additional scanning of the spectrally encoded frame in the direction parallel to the spectrally encoded line, the full color of the specimen could be acquired without changing the basic configuration of the imaging probe. Moreover, by scanning at sufficiently small steps, the full spectrum of the emitted light could be computed for each point on the sample, producing a three-dimensional spectral cube with a spectral resolution which equals that of the imaging system. At certain system configurations and illumination parameters, this technique would allow capturing spectral cubes with sensitivities that could potentially exceed those of current state-of-the-art point-scanning and line-scanning techniques.

2. Experiment

Our bench top spectrally encoded spectral imaging (SESI) system (Fig. 1) consisted of a single spectrally encoded collection channel and a separate broadband illumination [21]. Sample illumination was carried out using an incoherent broadband source (Halogen and Mercury lamps) coupled into a fiber bundle light guide whose distal end was positioned approximately 5 mm away from to the sample surface. At this configuration, we estimate that less than 1% (3 mW) of the total illuminating power was overlapping with the spectrally encoded imaging line. Alternatively, a beam from a spatially coherent supercontinuum source (Fianium Inc. SC-400-4) was focused onto a transverse line on the sample by first focusing the beam onto a galvanometric scanner (GS) using an achromatic lens (L3, 125 mm focal length), and imaging the focused spot using a 2f-2f configuration with a cylindrical lens (CL, 100 mm focal length). In order to reduce coherent speckle noise, the galvanometric scanner was actuated by a sinusoidal waveform at frequency that equaled half of the line acquisition rate, allowing for 12° angle scan during each line exposure.

Light scattered from the sample was collected by an imaging lens (L1, 25 mm focal length, 25 mm diameter), diffracted by a transmission grating (G, 1200 lines/mm, Wasatch Photonics Inc.) and focused into the core of a single-mode optical fiber (SMF, Nufern, S405-HP) using an achromatic lens (L2, 40 mm focal length). The spatial interval δx along the wavelength axis at the center field of view was then related to the corresponding wavelength interval $\delta\lambda$ according to [22] $\delta x = Gf\delta\lambda/\cos\theta_0$, where G denotes the grating groove density, f denotes the focal length of the imaging lens (L1) and θ_0 denotes the Littrow's angle.

#141151 - $15.00 USD Received 14 Jan 2011; revised 6 Mar 2011; accepted 6 Mar 2011; published 25 Mar 2011

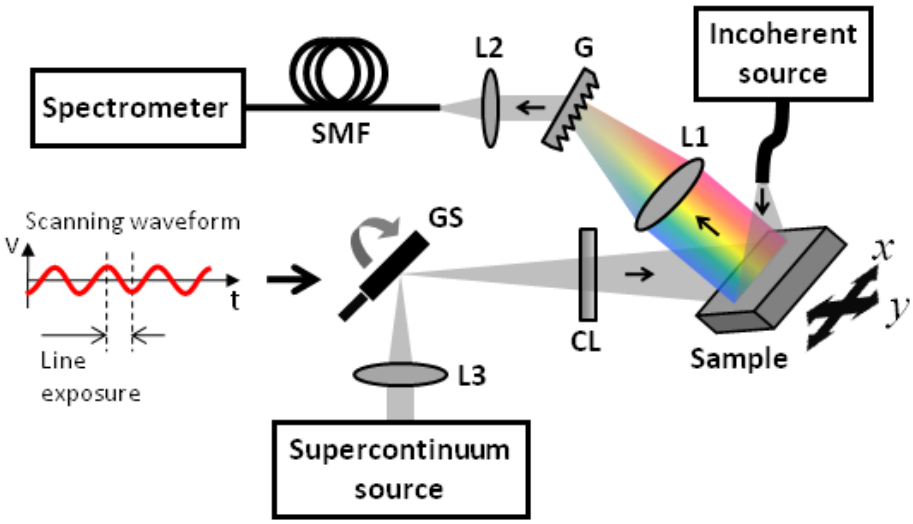

Fig. 1. Schematic drawing of the spectrally encoded spectral imaging system. L1, L2, L3 – achromatic lenses, CL – cylindrical lens, G - transmission diffraction grating, GS – galvanometric scanner, SMF – single mode fiber.

The light emanating from the optical fiber was collimated by an objective lens (Leica, Achro, 0.1 NA) and directed into a spectrometer comprised of a 1800 lines/mm transmission diffraction grating (Wasatch photonics Inc.), a multi-element lens (Nikon AFC, 50 mm focal length) and a high sensitivity back-illuminated electron multiplication charged coupled device (EMCCD) camera (Andor Technology plc., DU970N-BV). High spectral acquisition rates (up to 1300 spectra per second) were accomplished by using a crop of ten lines of the EMCCD. The optical configurations at both ends of the fiber were optimized for high transmission efficiency at 450-650 nm, with the wavelength of 550 nm diffracting at Littrow's angles.

Three dimensional spatial-spectral data cubes were obtained by scanning the sample laterally using two motorized translation stages, where the fast (y) axis was used to obtain a two-dimensional "monochrome" image, and the slow (x) axis scanning was used to obtain the spectral information. At this configuration, each point on the sample is sequentially imaged by monotonically increasing wavelengths within the total illumination bandwidth. The highest possible spectral resolution $\Delta\lambda_{max}$ is thus equal to the width of the point-spread function (PSF) of the system in wavelength units [22]:

$$\Delta\lambda_{max} = 1.029\frac{\lambda\cos\theta_0}{DG}, \tag{1}$$

where D denotes the effective diameter of the imaging lens L1. In order to ensure optimal sampling of the spectrum, the shift of the spectrally encoded frames along the x axis Δx_s should not exceed one half of the spatial resolution: $\Delta x_s \le 0.5\lambda f/D$. In a confocal configuration of the spectrally encoded system, in which the illumination PSF is similar to the imaging PSF, both spectral and spatial resolutions would be approximately 35% higher than those of non-confocal systems [22], hence requiring 35% smaller sampling steps along the x axis.

3. Results

In order to demonstrate spectrally encoded color imaging using a single collection fiber, three two-dimensional images of a black-on-white USAF-1951 scattering resolution target were captured while the sample was translated along the wavelength (x) axis between successive frames (Fig. 2a). The three gray-scaled images were first normalized by dividing each

#141151 - $15.00 USD Received 14 Jan 2011; revised 6 Mar 2011; accepted 6 Mar 2011; published 25 Mar 2011

spectrally encoded line by a reference spectrum which was acquired by imaging a single line of the white portion of a color calibration chart. The normalized images were then color-coded digitally using the corresponding RGB values for each encoding wavelength, and were summed to form a composite color image (Fig. 2a). At its central part, the composite image contained three principle colors that allowed the measurement of the actual (white) color of the resolution target. However, at the edges of the composite image, not all three monochromatic wavelengths were present for each point, resulting in colors which are biased toward blue and red hues at the right and left hand parts of the image, respectively. The effective color gamut of the image at the locations marked by dashed, solid and dotted arrows in Fig. 2a, are drawn on a CIE-xy chromaticity diagram using solid, dashed and dotted triangles, respectively (Fig. 2b). Compared with the gamut of the sRGB standard color space used by many commercial display devices (marked by a gray triangle) the composite color image has equivalent color range, with the exception of the leftmost part of the image which lacks blue hues, showing noticeable bias toward yellow.

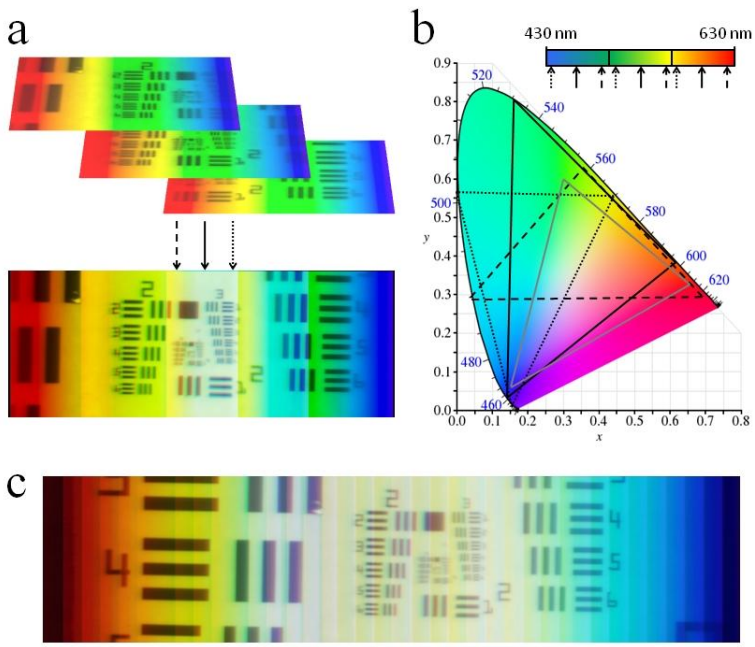

Fig. 2. Spectrally encoded color imaging through a single collection channel. (a) Three laterally translated color-coded frames added to produce a color image of a black-on-white printed resolution target. (b) A CIE-xy diagram with three color gamut triangles corresponding to different spatial lines in the resolution target, marked by the dashed, solid, and dotted arrows in (a). The color gamut of the standard sRGB color base is marked by a gray triangle. (c) A color image of the resolution target, assembled from thirty wavelength-encoded frames which were gradually translated in the wavelength (x) axis.

While three wavelengths at the blue, green and red parts of the spectrum would be sufficient for color imaging in a spectrally encoded imaging system [20], additional spectral information could be obtained by capturing a higher number of frames separated by smaller displacements along the x-axis. A composite image of 30 raw images of the test target is shown in Fig. 2c, for which the target was moved by steps of 0.48 mm in the wavelength (x) axis between frames, corresponding to approximately 14 nm steps in the encoding wavelengths of each point. Without any color adjustment, the central region of the white resolution target had a slight yellowish hue, which is attributed primarily to inaccuracies in our spectral normalization algorithms at the edges of each individual frame and to the nonlinearity of the diffraction angle with respect to wavelength. Note that while the true white

#141151 - $15.00 USD Received 14 Jan 2011; revised 6 Mar 2011; accepted 6 Mar 2011; published 25 Mar 2011

color of the target was not fully recovered at the edges of the composite image, the image could still reveal spatial features of the resolution target, albeit with strong color casts due to the missing parts of the spectrum. Evidently, additional scanning in the x axis would increase the total field of view, and consequently the region in which accurate color could be reproduced. Moreover, by decreasing the lateral steps between acquisitions, spectral resolution could be as high as $\Delta\lambda_{max}$ (Eq. (1). As a result, the data collected from each point on the sample would contain not only its perceived color, but also the full spectrum of the scattered light.

In order to demonstrate high resolution spectral imaging using spectral encoding, we imaged a color pattern printed on a white paper using a commercial color inkjet printer (Fig. 3). The three-dimensional raw data cube (Fig. 3a) contained 73 monochromatic (16 bit) 1600 (x) by 500 (y) pixel frames which were gradually shifted in the x axis by 0.25 mm, corresponding to approximately 9 nm shifts of the encoding wavelengths. Exposure time for each encoded line was 1 ms, resulting with a total exposure time of 36.5 s for the entire data cube. A single y-λ cross-sectional plane through the data set (Fig. 3b) contained the full spectra emitted from each point along the dashed white line in Fig. 3a. Two reflection spectra, corresponding to blue (solid curve) and red (dashed curve) color spots of the printed image are shown in Fig. 3c. For visualization of the actual color of the sample, the data was collapsed onto a 1600 × 500 × 3 matrix by calculating the projection of the acquired spectra onto the three RGB vectors (Fig. 3d). For comparison, a photograph of the printed pattern using a digital camera is shown in Fig. 3e, where the white regions of the paper outside the field of view were used for white balance calibration.

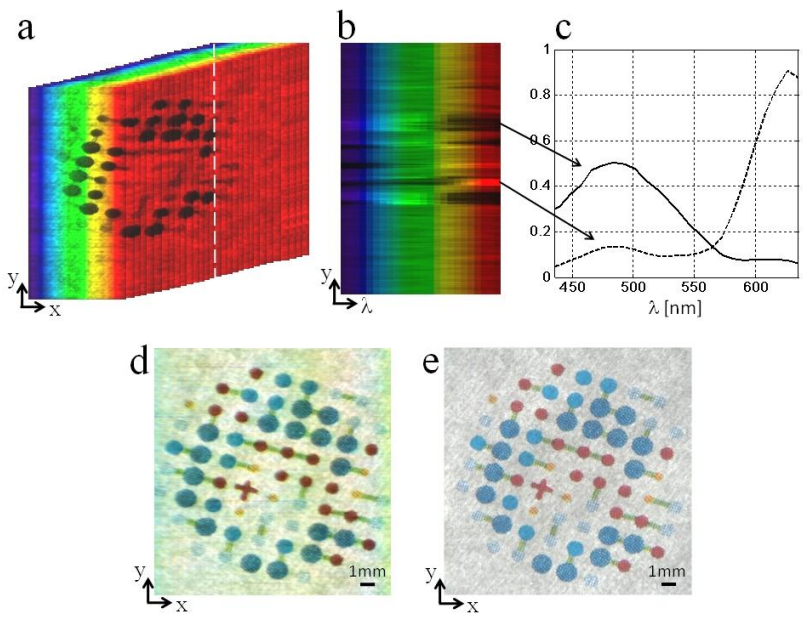

Fig. 3. Spectrally encoded spectral imaging of a color pattern printed on a white paper. (a) The spectral color-coded raw data structure. (b) A cut through the raw data across the plane marked by a dashed white line in (a). (c) Spectral response of two selected points in the object, where each spectrum contained 24 discrete wavelengths. (d) A reconstructed color image of the sample. (e) A photograph of the sample captured with a digital camera.

Using spatially coherent light, one can increase the signal efficiency of SESI by using higher illumination irradiance. In order to demonstrate SESI using spatially coherent illumination, approximately 10 mW from the supercontinuum source were focused by a cylindrical lens (see Fig. 1) to illuminate a broadband line on the sample, which was wider (20 μm) and slightly longer (12.8 mm) than the 1 μm × 10 mm spectrally encoded line. The

#141151 - $15.00 USD Received 14 Jan 2011; revised 6 Mar 2011; accepted 6 Mar 2011; published 25 Mar 2011

spectral data cube of a green leaf attached to a microscope slide (Fig. 4) was digitally assembled from 65 spectrally encoded frames, repeatedly shifted by 0.2 mm along the wavelength (x) axis, corresponding to spectral sampling intervals of approximately 6.5 nm. Exposure time was 50 ms per line, resulted in 20 s exposure per single frame and a total of 11 m for the entire data set. A color image of the leaf, reproduced by projecting the acquired spectra onto the three RGB vectors, is shown in Fig. 4a. A photograph of the leaf acquired by a digital camera is shown in Fig. 4b as reference, in which the white background was used for white balance calibration. The measured spectrum from the region marked by a white circle in Fig. 4a is plotted in Fig. 4c (solid curve) and compared with a spectrum measured from the same region using a commercial spectrometer (Ocean Optics Inc. USB4000). A good overlap between the two spectra is evident in the wavelength range of 480 nm to 650 nm, where the deviation between the spectra below 480 nm is attributed to the low SNR at this part of the spectrum, caused by the combined effect of the low source power below 450 nm, low diffraction efficiency of the gratings below 480 nm, and the low reflection of the leaf at this wavelength range.

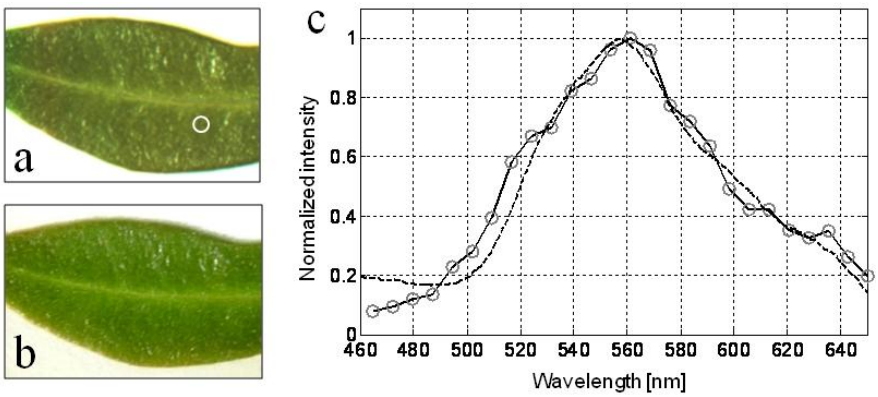

Fig. 4. (a) Color image of a green leaf obtained by projecting the SESI spectral data onto RGB values. (b) A photograph of the leaf in (a) captured by a digital camera. (c) A spectrum of the region encircled in (a) (solid line), compared with a spectral measurement of the same region using a commercial spectrometer (dashed line).

4. Signal-to-noise ratio

The ability to conduct spectral imaging could be a useful feature in any future spectrally encoded endoscopic system. The main advantage of this approach is that the SEE imaging probe does not need to be changed; it could still acquire gray-scale reflectivity images with high sensitivity (80 dB [23]). For color and spectral imaging at low spectral resolutions, the SNR of the integrated image would not drop significantly since the shorter acquisition time frames would be compensated by the acquisition of multiple images of the same regions. Applications which require high spectral resolutions are not expected to be limited by SNR, but rather by the accuracy of the scanning mechanism, the total acquisition time, and the data processing.

In SESI, the signal (in electrons) measured for each resolvable element (x,y,λ) is equal to $Q_e r\left(I_{\max} s/h\nu\right)t$, where Q_e denotes the detector quantum efficiency, r denotes sample reflectivity, $I_{\max}$ denotes the maximum permissible exposure (MPE) in units of W/cm^2, s denotes the area of a single spatial resolvable element, ν denotes the optical frequency, and t denotes the exposure time of a single resolvable element. When both the illumination and collection channels are spectrally encoded, each pixel in a single $N \times N$ pixel frame is sequentially illuminated by a single wavelength only, while the detection of the light reflected from that pixel is performed on a single detector during the entire exposure time given by

#141151 - $15.00 USD Received 14 Jan 2011; revised 6 Mar 2011; accepted 6 Mar 2011; published 25 Mar 2011

$t=\frac{T}{N}\frac{1}{N+M-1}$, where T denotes the total imaging time and M denotes the number of (spectral) resolvable elements in the wavelength axis. Assuming that dark current is the dominant noise source (neglecting shot noise and read noise) the SNR is given by ($N,M>>1$):

$$\mathrm{SNR}_{\mathrm{SESI}}=\frac{Q_e r\frac{I_{\max}s}{h\nu}\frac{T}{N}\frac{1}{N+M}}{\sqrt{D\frac{T}{N}\frac{1}{N+M}}}=\frac{Q_e r I_{\max}s\sqrt{T}}{h\nu\sqrt{D}}\sqrt{\frac{1}{N\left(N+M\right)}}\ , \tag{2}$$

where D denotes the dark current in electrons per second per pixel.

In comparison, when scanning the sample point-by-point with a tightly focused laser beam and measuring its spectrum to obtain a spectral image, the signal measured for each resolvable element (x,y,λ) is given by $Q_e\frac{r\left(I_{\max}s/h\nu\right)}{M}t_{p-p}$, where $t_{p-p}=T/N^2$ denotes the exposure time for a single pixel in point-by-point scanning. Assuming that dark current is the dominant noise source, the SNR for point-by-point spectral imaging is given by:

$$\mathrm{SNR}_{p-p}=\frac{Q_e\frac{r\left(I_{\max}s/h\nu\right)}{M}\frac{T}{N^2}}{\sqrt{D\frac{T}{N^2}}}=\frac{Q_e r I_{\max}s\sqrt{T}}{h\nu\sqrt{D}}\frac{1}{MN}\ . \tag{3}$$

When the sample is scanned by an entire focused line and the spectral cube is acquired by a two-dimensional CCD [5], each spatial pixel in the image could still be illuminated by irradiance $I_{\max}$, however the total exposure time would now be N-times longer than that of point scanning, thus the SNR for line-by-line spectral imaging is given by:

$$\mathrm{SNR}_{l-l}=\frac{Q_e\frac{r\left(I_{\max}s/h\nu\right)}{M}\frac{T}{N}}{\sqrt{D\frac{T}{N}}}=\frac{Q_e r I_{\max}s\sqrt{T}}{h\nu\sqrt{D}}\frac{1}{M\sqrt{N}}\ . \tag{4}$$

Assuming, for brevity, that the number of resolvable wavelengths is equal to the number of spatial resolvable elements ($M = N$) we finally obtain:

$$\mathrm{SNR}_{\mathrm{SESI}}:\mathrm{SNR}_{l-l}:\mathrm{SNR}_{p-p}=\frac{N}{\sqrt{2}}:\sqrt{N}:1\ , \tag{5}$$

implying that SESI has an SNR advantage over line-by-line and point-by-point scanning by a factor which equals $\sqrt{N/2}$ and $N/\sqrt{2}$, respectively. Note that the additional field of view at the edges of the SESI frame, which do not contain full spectral information, where not considered in the derivation of Eqs. (2) and (5).

The large advantage in SNR of SESI over other spatial scanning techniques, as reflected in Eq. (5), holds only when the illumination and the collection channels are both spectrally encoded. In specific configurations where one of the channels is not spectrally encoded, for example when using broadband widefield illumination as presented in the above experimental demonstration, the signal, and consequently the SNR, would be M-times smaller than that used in Eq. (2). One important consequence of this requirement is that SESI of fluorescent samples, although technically feasible, would not have any SNR advantage over existing spectral imaging techniques since fluorescence detection require either the illumination or the collection channels to be non-spectrally encoded [21,24,25]. Two other experimental factors

#141151 - $15.00 USD Received 14 Jan 2011; revised 6 Mar 2011; accepted 6 Mar 2011; published 25 Mar 2011

which may reduce the SNR advantage of SESI include the use of detection systems in which read noise or shot noise could not be neglected compared to the dark noise, and when imaging a specimen having an additional energy-dependant damage threshold (often provided in units of J/cm^2). In these cases, both SESI and line scanning would benefit less from their reduced illumination irradiance.

A direct SNR comparison between SESI and other methods that utilize variable color filters, wavelength swept sources, and low coherence interferometry, would largely depend upon the exact technological parameters of the imaging systems, and is beyond the scope of this work. In general, these approaches often rely on full-field sample illumination, and are thus expected to have a higher SNR, provided that the systems' speed and performance are not limited by the specific instrumentation (i.e. camera, variable filters, and light source) that is being used.

5. Discussion

Spectral imaging using spectral encoding provides a detailed analysis of a specimen using a single-mode imaging fiber. This technique could be implemented within a multi-channel spectrally encoded system (see Ref [21].) and in endoscopic systems with ultra-miniature imaging probes.

Unlike other spectral imaging methods, the spatial and spectral resolutions of SESI are directly linked; the maximum number of resolvable wavelengths is essentially limited by the number of resolvable points in a single frame. By controlling the lateral shift between frames, the user can chose an arbitrary wavelength sampling steps for balancing between spectral resolution and total acquisition time. Incorporated into a bench-top optical microscope or as a stand-alone imaging system, SESI could be designed to produce high spatial and spectral resolutions: neglecting optical aberrations, an imaging system comprised of 10 mm diameter objective lens, 1500 lines/mm diffraction grating and 400 nm source bandwidth, would be limited only by the number of available pixels of current state-of-the-art line-scan cameras (8192 pixels), resulting with submicron lateral resolutions and up to 0.05 nm spectral resolution. The broadband illumination source could be spatially incoherent, allowing for a versatile, speckle-free imaging, or spatially coherent, resulting in signal efficient imaging with higher SNR. Whereas SESI was demonstrated useful for capturing the spectrum of light scattered from a specimen, it could also be utilized for simultaneous imaging of multiple fluorescent labels [8], albeit at relatively low SNR [21].

For minimally invasive endoscopic applications, SESI enables effective color imaging using only a single collection channel. In contrast with the previously demonstrated approach for color SEE [20], SESI utilizes the entire spectrum for imaging and would allow color imaging without changing the basic probe configuration. Unlike the bench-top system, high resolution SESI would probably be more challenging within the constraints of a miniature spectrally encoded endoscope [26]. Clinical applications of endoscopic SESI would require slow scanning of the field of view along the wavelength (x) axis while continuously acquiring images. For example, using a 500 μm diameter endoscopic probe with 1500 lines/mm grating and 400 nm total source bandwidth, a full spectral (square) image would contain up to 960^3 data points with a maximum of 960 resolvable wavelengths. However, achieving such high spectral resolution would be extremely challenging due to the limited scanning accuracy and navigation of the distal end of the endoscope. Motion artifacts and the non-Cartesian geometry of the field of view [22] would also decrease the spectral resolution. One possible approach to reduce these effects would be to apply sophisticated image processing algorithms on the acquired sequence of images, which would identify specific patterns and compute the actual lateral shift of the field of view for the different parts of the image. The spectrum at each point in the image could then be retrieved at sampling wavelengths that would depend on the relative displacement between the probe and the tissue. Using such an approach would

#141151 - $15.00 USD Received 14 Jan 2011; revised 6 Mar 2011; accepted 6 Mar 2011; published 25 Mar 2011

require intensive data processing that would limit the ability to work in real time acquisition modes.

In summary, we have demonstrated a new method for conducting color and spectral imaging using spectral encoding by scanning the two-dimensional spectrally encoded frame along the wavelength axis. This method was demonstrated by spectral imaging of a resolution test target, a color printed image and a live green leaf. Using spectral encoding at both the illumination and the collection channels, SESI would have an improved SNR over current point and line scanning techniques, and would provide spectral resolution which is limited only by the optical properties of the imaging optics.

Acknowledgements

The study was funded in part by the Israel Science Foundation grant (716/09) and by the European Research Council starting grant (239986).